Intracellular nanoscale architecture as a master regulator of calcium carbonate crystallization in marine microalgae

Yuval Kadan[a], Fergus Tollervey[b,c], Neta Varsano[d], Julia Mahamid[b,1], and Assaf Gal[a,1]

[a]Department of Plant and Environmental Sciences, Weizmann Institute of Science, Rehovot 7610001, Israel; [b]Structural and Computational Biology Unit, European Molecular Biology Laboratory (EMBL), Heidelberg 69117, Germany; [c]Faculty of Biosciences, Collaboration for joint PhD degree between EMBL and Heidelberg University, Heidelberg 69120, Germany; and [d]Department of Structural Biology, Weizmann Institute of Science, Rehovot 7610001, Israel

Edited by Jennifer Lippincott-Schwartz, Janelia Farm Research Campus, Ashburn, VA, and approved September 11, 2021 (received for review January 13, 2021)

Unicellular marine microalgae are responsible for one of the largest carbon sinks on Earth. This is in part due to intracellular formation of calcium carbonate scales termed coccoliths. Traditionally, the influence of changing environmental conditions on this process has been estimated using poorly constrained analogies to crystallization mechanisms in bulk solution, yielding ambiguous predictions. Here, we elucidated the intracellular nanoscale environment of coccolith formation in the model species *Pleurochrysis carterae* using cryoelectron tomography. By visualizing cells at various stages of the crystallization process, we reconstructed a timeline of coccolith development. The three-dimensional data portray the native-state structural details of coccolith formation, uncovering the crystallization mechanism, and how it is spatially and temporally controlled. Most strikingly, the developing crystals are only tens of nanometers away from delimiting membranes, resulting in a highly confined volume for crystal growth. We calculate that the number of soluble ions that can be found in such a minute volume at any given time point is less than the number needed to allow the growth of a single atomic layer of the crystal and that the uptake of single protons can markedly affect nominal pH values. In such extreme confinement, the crystallization process is expected to depend primarily on the regulation of ion fluxes by the living cell, and nominal ion concentrations, such as pH, become the result, rather than a driver, of the crystallization process. These findings call for a new perspective on coccolith formation that does not rely exclusively on solution chemistry.

biomineralization | coccolith | crystallization | cryoelectron tomography | ocean acidification

In the ocean, many geochemical cycles are driven by the activity of microorganisms, linking global environmental processes to fundamental cell biology. An important sink for the long-term sequestration of carbon in deep-sea sediments is biogenic calcium carbonate crystals produced by coccolithophores, microalgae that cover their cells with mineralized scales called coccoliths (1). Although it is established that coccoliths form intracellularly within specialized vesicles, the local chemical conditions within the cell, which facilitate this pH-sensitive crystallization process, are unknown (2, 3). Our poor understanding of the biomineralization process poses major challenges when trying to predict how future changes to seawater chemistry, most notably ocean acidification, will affect coccolithophore physiology (4).

A coccolith is a composite structure made of a radial array of calcite crystals that nucleate and grow on the rim of a preformed organic base plate (Fig. 1 *A* and *B*). Each coccolith forms inside a Golgi-derived compartment, the coccolith vesicle. Several studies have elucidated the cellular anatomy of coccolith formation in a few key species (5–9). In the model species *Pleurochrysis carterae*, calcium ions are transported to the coccolith vesicle in complex with polysaccharide counter ions, forming dense membraneless particles, called coccolithosomes (Fig. 1*C*) (7). Traditionally, the calcite crystals of coccoliths were thought to form by a solution-mediated growth mechanism (6), where the crystals grow from a supersaturated solution within the coccolith vesicle (10–12). This notion stems from structural investigations that relied on electron microscopy of chemically fixed and resin-embedded cells. However, it is well known that such procedures alter fine structures within the cell (13). It is very challenging to investigate in vivo the cellular mechanisms that control crystallization. Specifically, the nanoscale environment inside the coccolith vesicle and how it affects the crystallization process remains elusive. As a consequence, the possible involvement of transient mineral phases and the influence of the confined volume of the coccolith vesicle on the chemistry of the process constitute major open questions.

In recent years, multiple alternatives to the solution-mediated ion-by-ion crystal growth process have been identified (14–17). It is now established that crystals can grow via a myriad of possible routes, involving various intermediate phases, which open almost limitless options for the crystallization pathway and its regulation (18). A well-known strategy in living systems is to use transient amorphous precursors that can be molded into intricate morphologies. Such processes are characterized by a confined environment, usually delimited by lipid membranes (14). The nanoscale effects of such confined

Significance

Some organisms evolved an extraordinary ability to control the formation of inorganic crystals. This is usually attributed to the localization of biomineralization processes to specialized and controlled cellular environments. However, traditional techniques are incompatible with investigations of precipitation reactions in vivo, and the structural determinants of these processes remain elusive. Here, we use state-of-the-art cryoelectron tomography to visualize with nanometer-scale resolution calcite formation by microalgae. The native-state structural data open a window into the microenvironment in which crystals form in vivo and shed light on the biological controls over the chemical precipitation process. These rapidly developing cryoelectron microscopy modalities hold promise to elucidate diverse phenomena at the interface between cells and their environment.

Author contributions: Y.K., J.M., and A.G. designed research; Y.K., F.T., and J.M. performed research; Y.K., F.T., N.V., and J.M. analyzed data; and Y.K., J.M., and A.G. wrote the paper with input from all authors.

The authors declare no competing interest.

This article is a PNAS Direct Submission.

[1]To whom correspondence may be addressed. Email: julia.mahamid@embl.de or assaf.gal@weizmann.ac.il.

This article contains supporting information online at http://www.pnas.org/lookup/suppl/doi:10.1073/pnas.2025670118/-/DCSupplemental.

Published November 11, 2021.

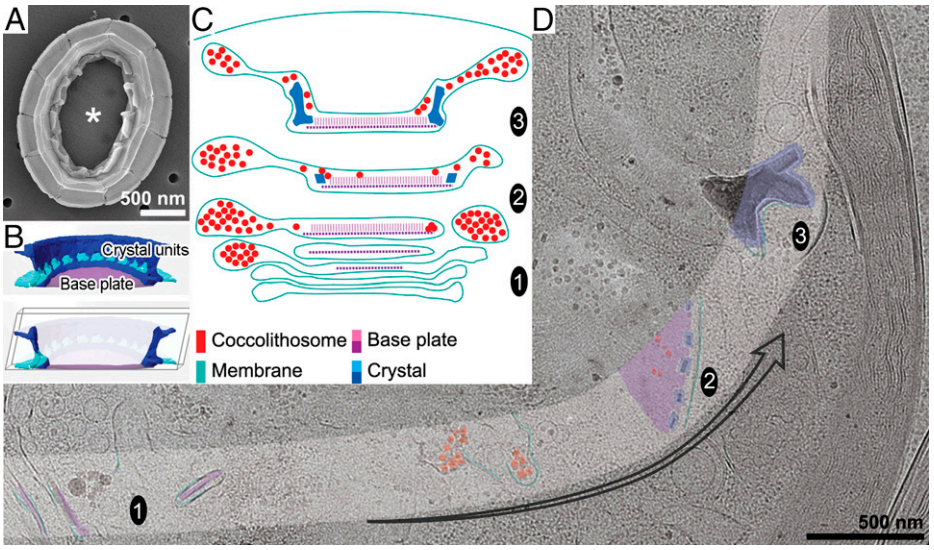

Fig. 1. In-cell cryo-ET reveals the native-state anatomy of coccolith formation in *P. carterae*. (*A*) Scanning electron microscope image of an isolated coccolith. The organic base plate (*) is indicated. (*B*) Schematic representations of the ultrastructure of a coccolith cut in half, showing the alternating interlocked crystals and the base plate. The lower scheme highlights the characteristic cross-sectional view, usually seen in thin lamellae. (*C*) A scheme indicating the three major stages reported in this work: 1) assembly of the coccolith vesicle, coccolithosomes, and base plate in the Golgi; 2) crystal nucleation and growth; 3) morphogenesis. (*D*) A cryo-TEM image of a subcellular area in a FIB-milled cell that contains multiple intracellular stages of coccolith formation. Selected features are artificially colored in the highlighted area using the color code in *C*.

volumes were shown to affect stabilization of mineral phases and polymorph selection during crystallization in vitro (19), suggesting that biomineralization processes can deviate significantly from the expectations of a solution-mediated process.

Here, we used in-cell cryoelectron tomography (cryo-ET), which provides native-like state, three-dimensional (3D), subnanometer scale information (20–22), to directly investigate the cellular nanoenvironment in which the coccolith crystals grow. The results show an orchestrated sequence of controlled interactions between the inorganic crystals and the organic scaffolds that shape their environment. We suggest that the main feature that funnels the crystallization process into its prescribed outcome is the confined volume in which the crystals grow.

Results

Actively calcifying cells of *P. carterae* were vitrified by plunging into liquid ethane without any chemical treatment. We used cryo–Focused Ion Beam (FIB) milling to generate ∼200 nm thin lamellae that traversed the entire width of the cell (*SI Appendix*, Fig. S1) (23). The cell anatomy of *P. carterae* proved advantageous, as several intracellular coccoliths form simultaneously in close proximity to each other (8). This enabled us to collect multiple datasets spanning the entire process of coccolith formation from a single lamella (Fig. 1*D*). Even though cryo-ET on FIB-milled lamellae is a relatively low-throughput technique, the breadth of data yielded enough snapshots of the process to allow us to derive a timeline of coccolith formation (*SI Appendix*, Fig. S2).

The early stages of coccolith formation are known to occur within the trans-Golgi (6, 7). Initially, a cellulosic fibrous scaffold (24), constituting the rigid layer of the base plate is assembled in a radial fashion (Fig. 2 *A* and *B*, in purple). Several such scales are seen simultaneously, in parallel to the appearance of coccolithosomes as dense particles (Fig. 2 *A* and *B*, in red). In Golgi cisternae, the coccolithosomes appear as an interconnected, particulate mass, whereas inside the coccolith vesicles they are arranged as individual spheres. In about half of the inspected cells, fibers are observed close to the forming coccolithosomes (Fig. 2*C*, in pink). We speculate that these fibers might be the charged polysaccharides that drive the condensation of this Ca-rich dense phase (5). Interestingly, the coccolithosomes and base plates are often seen in the same vesicle even before the initiation of calcite nucleation, suggesting a temporal regulation of crystallization activation (Fig. 2 *A* and *B*). Dense membrane-bound organelles, which are structurally similar to the Ca-P-rich bodies of coccolithophores (25), are present in the cytoplasm of the cells (Fig. 2*H*). In accordance with previous reports, we never observed a physical connection between the Ca-P-rich bodies and the Golgi cisternae that contain coccolithosomes. This points to an indirect ion transport pathway between these two calcium stores (26, 27).

After the coccolith vesicle leaves the Golgi, the base plate changes dramatically, developing into a multilayer organic structure. In addition to the flat horizontal layers (28), a layer of vertical fibers covering the surface of the base plate interior is observed (Fig. 2 *D* and *E*, in light purple and Movie S1). The vertical fibers create a gel-like volume, denser at the center of the base plate and gradually disappearing toward the periphery (Fig. 2*F*). This gel-like environment, where the fibrous material takes ∼5% of its volume, can physically or chemically constrict the upcoming crystallization process to the spatially confined nanoenvironment of the base plate periphery. These fibers were observed in later stages of coccolith formation but were absent in extracellular coccoliths (*SI Appendix*, Fig. S3). Furthermore, we observed at the periphery of the base plate a bulky dense phase, morphologically distinct from both a crystal and the coccolithosomes (Fig. 2 *D* and *E*, in dark red). Such a localized Ca-rich phase was demonstrated to form in vitro at the base plate rim as the result of specific interactions between soluble polysaccharides and the base plate (29, 30) and can serve as a precursor that facilitates crystal nucleation (31). It is worth noting that crystallization was never detected in areas where the perpendicular fibers were present, pointing to an inhibitory effect of the fibrous gel-like volume on crystal growth.

In many datasets, the coccolith vesicle membrane is decorated with a layer of densities on its luminal side (Fig. 2 *D* and *G*, yellow arrows). The appearance of these membrane

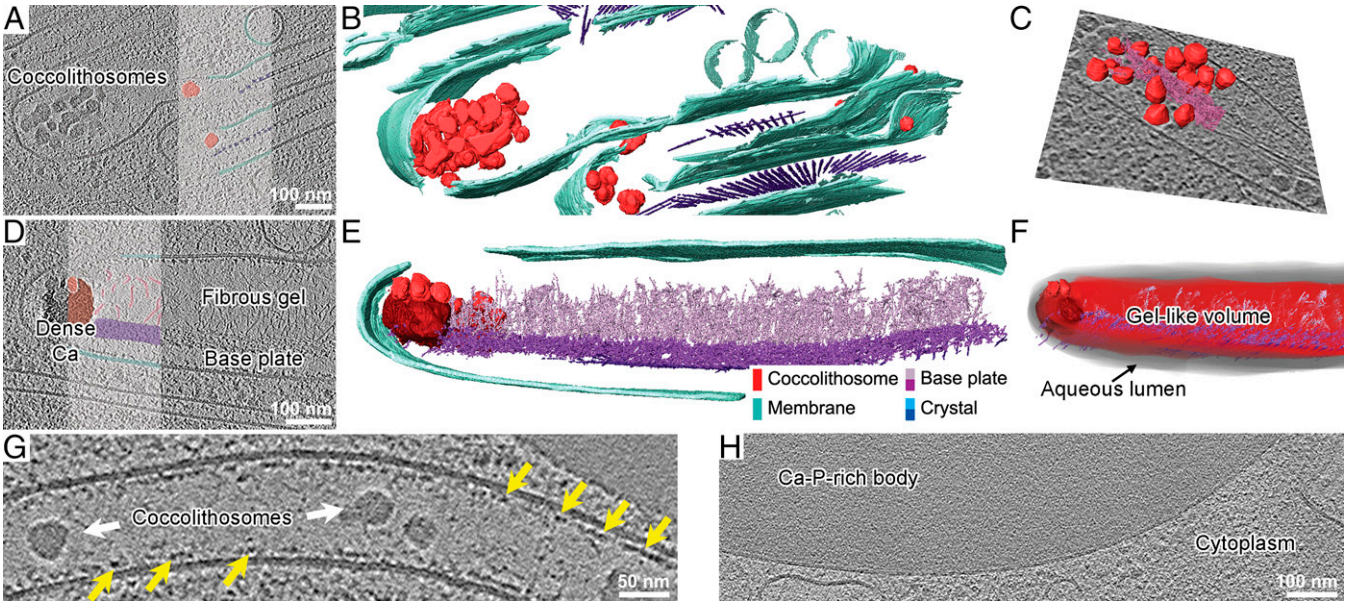

Fig. 2. The base plate architecture shapes a confined nano-environment within the coccolith vesicle. (*A–C*) The trans-Golgi region, where the organic scales are assembled. (*D–F*) A mature base plate inside a coccolith vesicle. (*A* and *D*) Slices in the reconstructed 3D volumes; some of the features in the highlighted rectangles are artificially colored according to the color code in *E*. (*B* and *E*) Three-dimensional surface rendering of segmented volumes. (*C*) Distinct fibers (partially segmented in pink) in close proximity to coccolithosomes (in red). (*F*) A 3D representation (gray) of the "free" solution volume inside the coccolith vesicle, which is limited by the vesicle membrane and the base plate gelatinous volume. (*G*) An extension of a coccolith vesicle that clearly demonstrates a dense array of complexes (yellow arrows) on the membrane luminal side. (*H*) A Ca-P-rich body within a cell. Its dense homogenous content is delimited by a membrane.

densities on the coccolith vesicle membrane correlates with the initial crystal growth stages: they were absent in vesicles containing the base plate only and observed when coccolithosomes were present in the vesicle. This might indicate that the array of membrane-associated molecular complexes is involved in the crystallization process. The dimensions of these complexes, about 19 nm high and 9.5 nm in diameter (*SI Appendix*, Fig. S4), are comparable to the sizes of known molecular machines, such as ATP synthases that measure ~20 × 10 nm (32). Even though we attempted to use subtomogram averaging to extract structural information of these complexes, their structures did not converge to a unique category. This suggests that there is more than one type of such molecular complexes, which could not be disentangled by 3D classification.

The preservation of the cellular fine structure allowed us to detect the interaction of minute crystals, only tens of nanometers in each dimension, with the base plate (Fig. 3 *A–C* and Movie S2). Previously, control of crystal orientation was hypothesized to originate from direct stereochemical interactions, presumably with a "ribbon" that arises from the base plate surface and tethers the crystals in a specific geometry that results in the alternating orientation of the crystals (1, 6, 33). No such ribbon was observed in the three datasets containing 11 minute crystals, and none of the crystallographic faces of the crystals is in contact with a defined structural feature. Instead, they nucleate about 50 nm from the edge of the base plate, oriented with one of their edges facing the base plate plane (Fig. 3*C*). The mechanism underlying the exquisite nucleation control of coccolith crystals still awaits elucidation.

The initial crystals exhibit the characteristic rhombohedral facets of calcite (Fig. 3 *A–C* and *SI Appendix*, Fig. S5). It remains unclear whether and how the bulky amorphous phase that was described earlier (29), and observed in Fig. 2*D*, may give rise to the nascent crystals. As the crystals grow, their morphology roughens and includes serrated surfaces with coccolithosomes adjacent to them (Fig. 3 *D* and *E* and Movie S3). In these maturation stages of coccolith formation, smooth and flat crystal facets, which are typical for ion-by-ion growth, are always observed in addition to the more complicated curved morphologies (Figs. 3 *D* and *E* and 4). Although the involvement of particle attachment is a hallmark of many biological crystal growth processes (34), here, coccolithosomes are exclusively seen outside the growing crystals, with the exception of the occasional appearance of voids of the same size within the crystals (Fig. 3*D*, yellow arrows). Quantitative analysis of the diameter of coccolithosomes as a function of their distance from the closest crystal face shows a decrease in particle size near growing crystals (Fig. 3*F*). We interpret these observations as the outcome of a complex process, in which coccolithosomes transport calcium to the growing crystal faces, where they undergo dissolution to support ion-mediated growth. Occasionally, a coccolithosome is engulfed by the crystal before the calcium ions are released from the polysaccharides, leading to the entrapment of its polysaccharides, and possibly water molecules, inside the crystal, leaving characteristic lower-density voids.

In the final stages of coccolith formation, the crystals attain their intricate shapes. It was postulated that coccolith crystal morphology is a manifestation of different crystallographic planes (6, 35, 36). Our observations demonstrate a more complex scenario, in which only the planes facing the interior of the coccolith vesicle or those formed by the meeting of two crystals exhibit smooth crystallographic features (Fig. 4 *A* and *B* and Movie S4). In all other directions, where the crystals grow toward the vesicle membrane, their morphology mirrors its shape (Fig. 4 *C*, *E*, and *F* and Movie S5). Such curved surfaces in other biominerals are commonly the result of a precursor mineral phase that exhibits a granular morphology (37). However, here, such surfaces are smooth to the nanometer scale (Fig. 4*C*). We observe a belt formed from ~2.5 nm diameter fibers of unknown composition surrounding the coccolith vesicle (*SI Appendix*, Fig. S6). These fibers may serve as cellular regulators of the shape of the vesicle membrane. Analysis of the distances from each point on the crystal surface to the

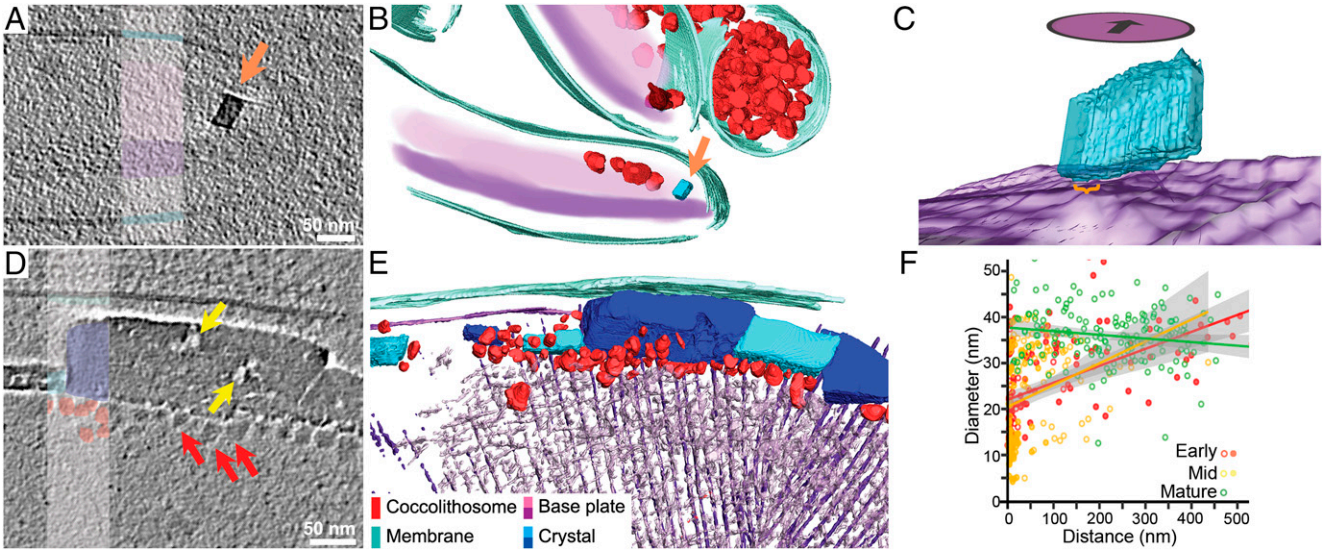

Fig. 3. Coccolith crystals nucleate with minimal contact with the base plate and grow via dissolution of coccolithosomes. (*A*–*C*) The smallest crystal observed. (*D* and *E*) A coccolith at a more advanced state. (*A* and *D*) Tomographic slices. Features in the highlighted rectangles are artificially colored, using the color code in *E*. In *D*, the red arrows point to coccolithosomes in spatial proximity to the crystals, and yellow arrows point to voids within the crystal. Voids with similar sizes were observed in about 75% of the crystals larger than 100 nm. (*B*, *C*, and *E*) 3D surface renderings of the datasets shown in *A* and *D*. (*C*) Grazing-angle view of the crystal in *A* from the interior of the base plate (perspective schematically shown by the purple ellipse). The closest region of the crystal to the base plate is highlighted in orange (~10 nm). (*F*) Analysis of coccolithosome sizes from five datasets as a function of the minimal distance to a crystal. In cases where the crystals are growing (two datasets of early stages in red and two datasets of intermediate stages in yellow), the slope of the linear regression is significantly different from the mature coccoliths (green). By an analysis of covariance; $P < 0.001$ for both contrasts, 95% confidence interval shown in gray.

closest point in the engulfing membrane shows that, throughout the growth process, the membrane is only tens of nanometers away from the crystal (Fig. 4*D*). Notably, at locations where crystal morphology is round and deviates from the crystallographic habit, the membrane is closer than 50 nm to the crystal, demonstrating the molding ability of the membrane and the highly confined space that is available for crystal growth.

In several instances, we observe a <20 nm thick dense phase covering the almost-mature crystals (Fig. 4*G*). This dense phase probably contains the soluble polysaccharides from the coccolithosomes that are excluded from the growing crystal, forming an organic sheath around mature crystals (8). In addition, coccolithosome-loaded vesicles fuse to the coccolith vesicle at sites where crystals grow in an outward direction, adding the necessary space for the elongation of the crystals (Fig. 4 *E* and *F*). Altogether, the tendency of the calcite crystals to express their crystallographic growth habit can be outweighed by membrane molding at close proximities. This directly substantiates the long standing hypothesis that the intricate crystal morphologies result from an interplay between both crystallographic and external driving forces.

Discussion

Studying biomineralization processes in situ at nanometer resolution is incompatible with most conventional experimental techniques (14, 38). Our in-cell cryo-ET approach, enabled by cryo-FIB specimen thinning, allowed the collection of extensive high-resolution native-like data from mineral-forming cells. This yielded a holistic "four-dimensional" view, which puts an emphasis on the nanoenvironment of the coccolith vesicle as a mechanistic driver of coccolith nucleation, growth, and morphogenesis. Our data indicate that the intricate shapes of the calcite crystals are the result of both the kinetics of ion-mediated growth that yields crystallographic planes and molding of crystal growth by the vesicle membrane that results in curved crystal surfaces.

When considering the well-established paradigm of an amorphous precursor pathway in biomineralization, the formation of coccoliths is still an undecided case. On the one hand, coccoliths exhibit intricate morphologies and precursor particles (the coccolithosomes), suggesting the involvement of amorphous phases. On the other hand, some of their surfaces show clear crystallographic facets, and the crystals do not demonstrate the granular crystal morphology that is indicative of a precursor transformation (34). Our in situ observations of coccolith formation reveal a fascinating variation of the known crystallization pathways, which combines both particle-mediated and ion-mediated crystal growth. In the case of coccoliths, the coccolithosomes as precursor particles are not incorporated to become an integral part of the growing calcite crystals but rather appear to function primarily in calcium transport.

An important open question is the transport mechanisms of calcium and carbonate ions to the coccolith vesicle. Our data, in accordance with previous observations confirming the presence of calcium in the coccolithosomes (13, 39), suggest that calcium ions are delivered to the coccolith vesicle via fusion of coccolithosome-loaded vesicles. It is unclear how calcium is transported to the coccolithosomes in the Golgi apparatus (27). The observation that other dense calcium stores such as the Ca-P-rich bodies are not spatially close to the coccolithosome vesicles points to additional transport stages (26). Regarding transport of carbonate, it is tempting to speculate that the presence of the molecular complexes on the coccolith vesicle membrane is related to the transmembrane transport of solutes (Fig. 2 *D* and *G*). If these are indeed membrane-bound transporters, they can be related to the import of inorganic carbon species from the cytoplasm, and their high density can account for the needed ion flux for crystallization.

Even though it is established that the environment inside the coccolith vesicle determines important chemical aspects of the crystallization process (10, 40–42), the lack of direct structural information had hampered attempts to quantitatively address

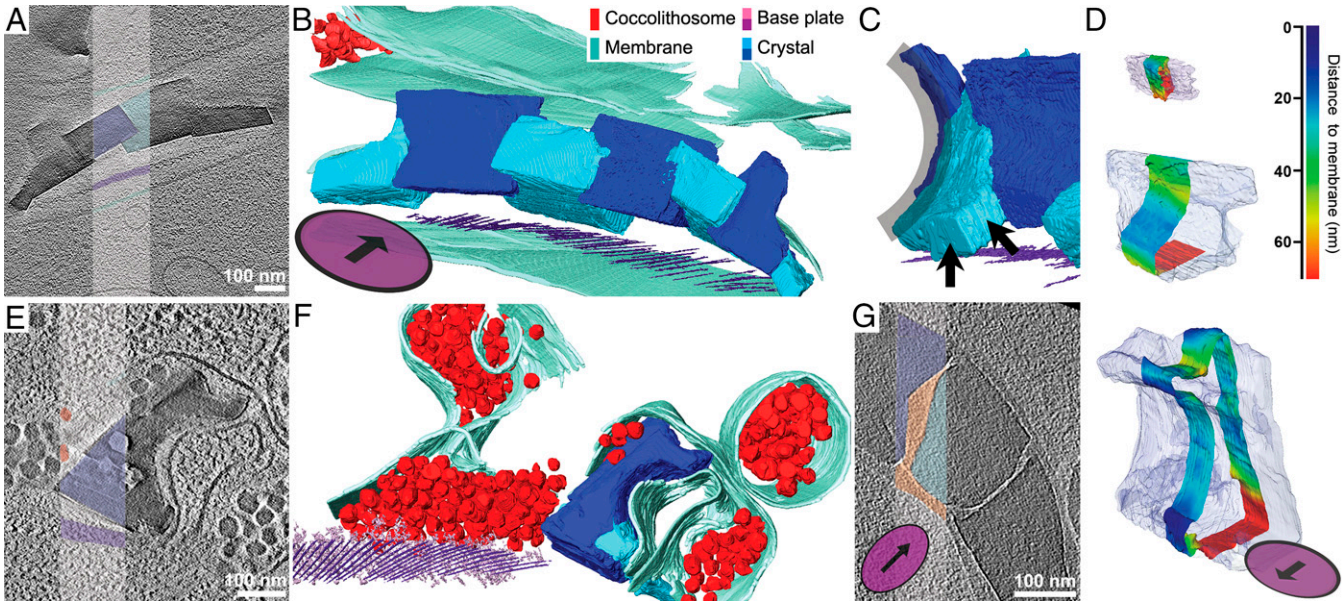

Fig. 4. The coccolith vesicle membrane shapes the growing crystals. (*A–C*) An intermediate growth stage before full expansion of the outermost elements, and (*E–G*) a coccolith at an almost mature stage. (*A* and *E*) Tomographic slices. Features in the highlighted rectangles are artificially colored, using the color code in *B*. (*B* and *F*) Three-dimensional surface renderings of the datasets shown in *A* and *E*, respectively. The purple ellipses in *B, D, G* schematically show the viewing angle relative to the base plate. (*C*) Side view of the coccolith in *A*; the curved distal surface is highlighted in gray, and the arrows indicate crystallographic facets. (*D*) Analyses of the distances from points on the crystal surface to the closest membranes. The analyzed crystals are the same as in Fig. 3*A* and in *A* and *E* here. (*G*) A dataset showing a distinct phase, which probably contains the constituents of the organic sheath, surrounding mature crystals (orange).

confinement effects. The 3D structural data generated in this work allowed us to calculate the volume fraction of the "aqueous lumen" within the coccolith vesicle (Fig. 2 *F*). This represents the volume inside the coccolith vesicle that is not occupied by the crystals, coccolithosomes, and fibrous macromolecules and therefore can facilitate solution-mediated crystal growth. Analysis of four datasets of early stage coccoliths showed that this "lumen" volume represents ~50% of the coccolith vesicle, which corresponds to ~0.36 μm^3. In such a volume, an uptake of two protons would reduce the nominal pH value from 8.2 to 7.8, similar to the projected acidification of the ocean at the end of the century (see *SI Appendix, Expanded Materials and Methods*). Such a nominal "pH decrease," triggered by the presence of two free protons inside the coccolith vesicle, emphasizes the caveats in using bulk terminology for confined volumes. On the one hand, the nominal pH change implies a significant influence on the crystallization process. On the other hand, it is not probable that two protons in the entire coccolith vesicle will have any substantial effect on crystal growth. We use this calculation to illustrate how solution chemistry characteristics, which represent thermodynamic driving forces in the bulk phase, become more complex to interpret in extreme confinement.

We expand such solution chemistry calculations to appreciate the extent of confinement within the coccolith vesicle. Fig. 5 demonstrates a scenario where only 100 nm separate the vesicle membrane from a rhombohedral calcite facet (in accordance with the analysis in Fig. 4*D*). The number of free calcium and carbonate ions in such a hypothetical solution are two orders of magnitude smaller than that needed to grow a single atomic layer of the crystal. In bulk solution diffusion is the primary mechanism to sustain the needed flux of ions for crystal growth, but within the confinement of the coccolith vesicle other mechanisms must be at work (43). We suggest two mechanisms that act in concert: First, the environment adjacent to the crystal is very different from a bulk solution, as many calcium ions are complexed by the negatively charged macromolecules (5), such that the activity of free ions is much lower than their actual concentration. Second, membrane transport of carbonate or bicarbonate ions can facilitate the rate of crystallization. Many chemical processes, including isotope fractionation, trace element incorporation, and the influence of environmental conditions on crystallization, are dependent on these nanoscale environment properties. For example, incorporation of trace elements such as boron, strontium, or magnesium cannot be explained by steady-state kinetics between the crystal surface and its neighboring solution, as the actual volume of the coccolith vesicle is too small to accommodate the needed trace

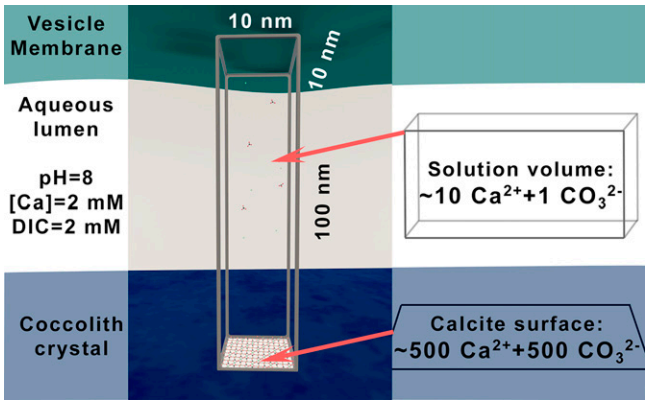

Fig. 5. Applying solution chemistry considerations to the coccolith vesicle. Calculations made for a calcite (104) face that is 100 nm away from the vesicle membrane. The aqueous lumen is modeled with a moderately supersaturated solution. A box of 10,000 nm^3 is used to demonstrate the ratio between soluble ions and ions at the crystal surface. In such a box, 100 nm^2 at the crystal surface accommodate ~1,000 ions, while the corresponding solution volume above it can accommodate about 10 free ions at any given time. DIC, dissolved inorganic carbon.

element concentration. It is therefore plausible that such reactions are controlled by fractionation events outside the coccolith vesicle, and crystallization acts as a final sink without substantial back-fluxes.

While *P. carterae* is a well-established model species for coccolith formation and proved advantageous for detailed imaging of the mineralization process, other species, including *Emiliania huxleyi*, are more abundant in the ocean and dominate the environmental effects of coccolithophores. Although differences between the cellular anatomies of these two species are known, most notably the absence of coccolithosomes in *E. huxleyi*, it is likely that the extreme confinement of the coccolith vesicle and the crystallization mechanism are similar and represent a conserved trait of coccolithophore calcification (1, 9). The current work emphasizes the roles of biological transmembrane transport mechanisms and chemical nanoenvironment. It thus points future research directions toward dissecting the cellular physiology of calcification as a primary target in understanding the varied influence of environmental conditions on different species.

Conclusions

Elucidating the nanoscale architecture of coccolith formation and the cellular confinement in which crystals form demonstrate how this crystallization process can significantly differ from crystal growth in solution. The presence of organic scaffolds, such as the base plate and the vesicle membranes, shapes the nanoscale conditions in a dynamic environment that evolves along the sequence of coccolith formation. It follows that, in order to maintain the needed chemical conditions inside the coccolith vesicle, the cell needs to regulate primarily ion fluxes in and out of this nanoenvironment, and the importance of the ion concentrations in this confined reaction volume is outweighed by these massive ion fluxes. Therefore, the effects of external changes, such as ocean acidification, may not directly affect the crystallization thermodynamics and kinetics within the coccolith vesicle but rather influence cellular homeostasis and impede the cellular regulatory mechanisms.

Materials and Methods

In brief (for detailed description, see *SI Appendix*), *P. carterae* cells grown in culture were decalcified by EDTA treatment and allowed to recalcify for a few hours. The actively calcifying cells were plunge-frozen on transmission electron microscopy (TEM) grids. Vitrified cells were milled using a cryo-FIB to generate about five 200 nm thin lamellae per grid. The grids were then transferred to a 300 kV Titan Krios TEM for acquisition of cryo-ET data. Tilt-series were aligned and reconstructed into 3D datasets. The datasets were segmented and visualized using dedicated software packages.

Data Availability. All study data are included in the article and/or supporting information. Tomograms depicted in the main figures are deposited to Electron Microscopy Data Bank (EMDB) under accession codes EMD-13755–EMD-13761.

ACKNOWLEDGMENTS. We are grateful to Ievgeniia Zagoriy, Wim Hagen, and the EMBL cryo-EM platform. This research was supported by the Israel Science Foundation (Grant No. 697/19) to A.G., EMBL, and the European Research Council (760067) to J.M.

1. J. R. Young, K. Henriksen, Biomineralization within vesicles: The calcite of coccoliths. *Rev. Mineral. Geochem.* **54**, 189–215 (2003).
2. A. R. Taylor, C. Brownlee, G. Wheeler, Coccolithophore cell biology: Chalking up progress. *Annu. Rev. Mar. Sci.* **9**, 283–310 (2017).
3. L. M. Mejía *et al.*, Controls over δ44/40Ca and Sr/Ca variations in coccoliths: New perspectives from laboratory cultures and cellular models. *Earth Planet. Sci. Lett.* **481**, 48–60 (2018).
4. J. Meyer, U. Riebesell, Reviews and syntheses: Responses of coccolithophores to ocean acidification: A meta-analysis. *Biogeosciences* **12**, 1671–1682 (2015).
5. M. E. Marsh, D. K. Chang, G. C. King, Isolation and characterization of a novel acidic polysaccharide containing tartrate and glyoxylate residues from the mineralized scales of a unicellular coccolithophorid alga *Pleurochrysis carterae*. *J. Biol. Chem.* **267**, 20507–20512 (1992).
6. M. Marsh, Coccolith crystals of *Pleurochrysis carterae*: Crystallographic faces, organization, and development. *Protoplasma* **207**, 54–66 (1999).
7. D. E. Outka, D. C. Williams, Sequential coccolith morphogenesis in *Hymenomonas carterae*. *J. Protozool.* **18**, 285–297 (1971).
8. P. van der Wal, E. W. de Jong, P. Westbroek, W. C. de Bruijn, A. A. Mulder-Stapel, Polysaccharide localization, coccolith formation, and Golgi dynamics in the coccolithophorid *Hymenomonas carterae*. *J. Ultrastruct. Res.* **85**, 139–158 (1983).
9. E. Paasche, A review of the coccolithophorid Emiliania huxleyi (Prymnesiophyceae), with particular reference to growth, coccolith formation, and calcification-photosynthesis interactions. *Phycologia* **40**, 503–529 (2001).
10. Y.-W. Liu, R. A. Eagle, S. M. Aciego, R. E. Gilmore, J. B. Ries, A coastal coccolithophore maintains pH homeostasis and switches carbon sources in response to ocean acidification. *Nat. Commun.* **9**, 2857 (2018).
11. H. Zhang *et al.*, An isotope label method for empirical detection of carbonic anhydrase in the calcification pathway of the coccolithophore Emiliania huxleyi. *Geochim. Cosmochim. Acta* **292**, 78–93 (2021).
12. C. S. Sikes, R. D. Roer, K. M. Wilbur, Photosynthesis and coccolith formation: Inorganic carbon sources and net inorganic reaction of deposition. *Limnol. Oceanogr.* **25**, 248–261 (1980).
13. Y. Kadan *et al.*, *In situ* electron microscopy characterization of intracellular ion pools in mineral forming microalgae. *J. Struct. Biol.* **210**, 107465 (2020).
14. S. Weiner, L. Addadi, Crystallization pathways in biomineralization. *Annu. Rev. Mater. Res.* **41**, 21–40 (2011).
15. S. Von Euw *et al.*, Biological control of aragonite formation in stony corals. *Science* **356**, 933–938 (2017).
16. Y. U. T. Gong *et al.*, Phase transitions in biogenic amorphous calcium carbonate. *Proc. Natl. Acad. Sci. U.S.A.* **109**, 6088–6093 (2012).
17. J. Aizenberg, D. A. Muller, J. L. Grazul, D. R. Hamann, Direct fabrication of large micropatterned single crystals. *Science* **299**, 1205–1208 (2003).
18. J. J. De Yoreo *et al.*, Crystallization by particle attachment in synthetic, biogenic, and geologic environments. *Science* **349**, aaa6760 (2015).
19. M. Zeng *et al.*, Confinement generates single-crystal aragonite rods at room temperature. *Proc. Natl. Acad. Sci. U.S.A.* **115**, 7670–7675 (2018).
20. J. Mahamid *et al.*, Visualizing the molecular sociology at the HeLa cell nuclear periphery. *Science* **351**, 969–972 (2016).
21. M. Beck, W. Baumeister, Cryo-electron tomography: Can it reveal the molecular sociology of cells in atomic detail? *Trends Cell Biol.* **26**, 825–837 (2016).
22. B. D. Engel *et al.*, In situ structural analysis of Golgi intracisternal protein arrays. *Proc. Natl. Acad. Sci. U.S.A.* **112**, 11264–11269 (2015).
23. M. Schaffer *et al.*, Optimized cryo-focused ion beam sample preparation aimed at in situ structural studies of membrane proteins. *J. Struct. Biol.* **197**, 73–82 (2017).
24. R. M. Brown, Jr, W. W. Franke, H. Kleinig, H. Falk, P. Sitte, Cellulosic wall component produced by the golgi apparatus of *Pleurochrysis scherffelii*. *Science* **166**, 894–896 (1969).
25. A. Gal *et al.*, Native-state imaging of calcifying and noncalcifying microalgae reveals similarities in their calcium storage organelles. *Proc. Natl. Acad. Sci. U.S.A.* **115**, 11000–11005 (2018).
26. A. Gal et al., Trace-Element Incorporation into Intracellular Pools Uncovers Calcium-Pathways in a Coccolithophore. *Adv. Sci.* **4**, 1700088 (2017).
27. H. Peled-Zehavi, A. Gal, Exploring intracellular ion pools in coccolithophores using live-cell imaging. *Adv. Biol.* **5**, e2000296 (2021).
28. J. M. Walker, B. Marzec, N. Ozaki, D. Clare, F. Nudelman, Morphological development of *Pleurochrysis carterae* coccoliths examined by cryo-electron tomography. *J. Struct. Biol.* **210**, 107476 (2020).
29. A. Gal *et al.*, Macromolecular recognition directs calcium ions to coccolith mineralization sites. *Science* **353**, 590–593 (2016).
30. L. Krounbi *et al.*, Surface-induced coacervation facilitates localized precipitation of mineral precursors from dilute solutions. *Chem. Mater.* **33**, 3534–3542 (2021).
31. A. Gal *et al.*, Templated and self-limiting calcite formation directed by coccolith organic macromolecules. *Chem. Commun.* **53**, 7740–7743 (2017).
32. N. Mnatsakanyan *et al.*, A mitochondrial megachannel resides in monomeric F_1F_O ATP synthase. *Nat. Commun.* **10**, 5823 (2019).
33. J. R. Young, J. M. Didymus, P. R. Brown, B. Prins, S. Mann, Crystal assembly and phylogenetic evolution in heterococcoliths. *Nature* **356**, 516–518 (1992).
34. A. Gal, S. Weiner, L. Addadi, A perspective on underlying crystal growth mechanisms in biomineralization: Solution mediated growth versus nanosphere particle accretion. *CrystEngComm* **17**, 2606–2615 (2015).
35. S. Mann, N. Sparks, Single crystalline nature of coccolith elements of the marine alga *Emiliania huxleyi* as determined by electron diffraction and high-resolution transmission electron microscopy. P. Roy. Soc. B-Biol. *Sci.* **234**, 441–453 (1988).
36. K. Henriksen, S. Stipp, J. Young, P. Bown, Tailoring calcite: Nanoscale AFM of coccolith biocrystals. *Am. Mineral.* **88**, 2040–2044 (2003).
37. I. Polishchuk *et al.*, Coherently aligned nanoparticles within a biogenic single crystal: A biological prestressing strategy. *Science* **358**, 1294–1298 (2017).

38. F. Nudelman *et al.*, The role of collagen in bone apatite formation in the presence of hydroxyapatite nucleation inhibitors. *Nat. Mater.* **9**, 1004–1009 (2010).
39. P. van der Wal, L. de Jong, P. Westbroek, W. de Bruijn, Calcification in the coccolithophorid alga *Hymenomonas carterae*. *Ecol. Bull.* **35**, 251–258 (1983).
40. L. Beaufort *et al.*, Sensitivity of coccolithophores to carbonate chemistry and ocean acidification. *Nature* **476**, 80–83 (2011).
41. M. D. Iglesias-Rodriguez *et al.*, Phytoplankton calcification in a high-CO_2 world. *Science* **320**, 336–340 (2008).
42. X. Yin *et al.*, Formation and mosaicity of coccolith segment calcite of the marine algae *Emiliania huxleyi*. *J. Phycol.* **54**, 85–104 (2018).
43. F. C. Meldrum, C. O'Shaughnessy, Crystallization in confinement. *Adv. Mater.* **32**, e2001068 (2020).